NIKOS MARTAKIS, LandTech Enterprises SA, Athens, Greece, AKIS TSELENTIS, and PARAKEVAS PARASKEVOPOULOS, Dept. of Seismology, University of Patras, Greece.

ID:646 High Resolution Passive Seismic Tomography- a NEW Exploration Tool for Hydrocarbon Investigation, Recent Results from a Successful Case History in Albania

Introduction

Listening to the earth passively over time and using the collected information can provide structural and lithologic information of the subsurface. The present passive seismic tomography (PST) survey, deals with the investigation of a known hydrocarbon field in S. Albania. The objective of this study is to use P and S-wave travel times from natural microearthquakes to derive 3D V_p (structural) and V_p/V_s (lithologic) information of the area.

In the hydrocarbon industry, seismicity has been mainly used as a reservoir monitoring tool for mapping fluid movements, faults (e.g. Maxwell et al., 1998), and hydraulic fracturing. Recently, Zhang et al., 2009, used the induced, by the production, seismicity to perform a reservoir 3D V_p and V_p/V_s tomography. During the past few years, PST has also been successfully applied for regional hydrocarbon exploration, thus showing its potential to map large regions for a relatively low cost, compared to conventional 3D seismic surveys (e.g.Martakis et al., 2006). Tselentis et al., 2006, showed that this method can even be applied at a local scale.

It is common knowledge that we will be always faced with exploration activity in geologically complex areas, such as fold and thrust belts. Exploration in these areas is challenging, as well as expensive and is driving the oil exploration industry towards the application of state of the art techniques. PST applications fall into the aforementioned category. The rationale for the application of tomography as a complimentary imaging tool is threefold. Firstly, it is a cost effective way to image a large area, where the terrain is difficult and as a consequence, conventional seismic is expensive and can be of poor quality due to seismic penetration problems. Secondly, the technique has the additional advantage of being environmentally friendly, which is an important consideration in all operational activities today. Third, by using the 3D velocity model derived from the PST and reprocessing existing seismic data (e.g. PSDM) we can drastically increase their resolution (e.g. Martakis et al., 2006).

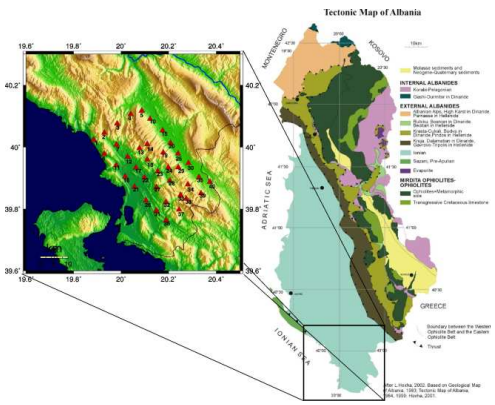

Fig.1 Geology & Seismological Network.

Data processing of PST data at a local scale for hydrocarbon exploration, is more complicated than simply applying off-the-shelf 3D inversion algorithms. To get the best resolution of the geological formations at the lowest cost, we tap an arsenal of technology: from initial velocity model selection to simultaneous earthquake hypocenter and 3D velocity-model and synthetic and real-data checkerboard tests.

Geology

The study area is located on the southeastern edge of Albania close to the border with Greece. The outcrop is dominated by large-scale linear folds, forming large anticlines and synclines, cut by major high-angle reverse faults. A major salt diapir in southern Albania is believed to

have protruded upwards from underlying thick Triassic salt. The Albanian orogenic belt trends NNW-SSE and lies between the Dinaric and Hellenic Alps (Fig. 1). It was built up by Alpine orogenic processes in the western Balkans area related to the plate convergence between Apulia and Eurasia and the closure of the Mesozoic Tethyan ocean. The Albanian orogenic belt represents a complex orogen made up of a heterogeneous tectonic nappe pile of Paleozoic, Mesozoic and Cenozoic domains.

Seismological Network and Data Processing

The designed network consisted of fifty 3-component 1-Hz LandTech LT100 borehole seismometers and 24-bit LandTech S24 recorders connected to a Global Positioning System (GPS) unit (Fig.1). The instruments have flat transfer function for velocity in the frequency range from 1 Hz to 100 Hz. The seismometers were buried in shallow 6m boreholes to improve the signal-to noise ratio.

We covered a plateau of an area of approximately 1000Km^2, where there is strong attenuation in conventional seismic reflection energy due to high velocity and/or karstified carbonate outcrop. Recording took place for a period of twelve months continuously, with a sampling frequency of 100 Hz.

The first stage in the analysis of the obtained seismological data is the automatic search for seismic events in the dataset of each station. Next, the selected events of all stations are cross-checked automatically and if an event is detected at more than 6 stations it is marked as a real event otherwise is eliminated from the data set. Finally, for each one of the seismograms we pick manually the P and S-wave phases using LandTech's passive seismic processing software PASEIS3.

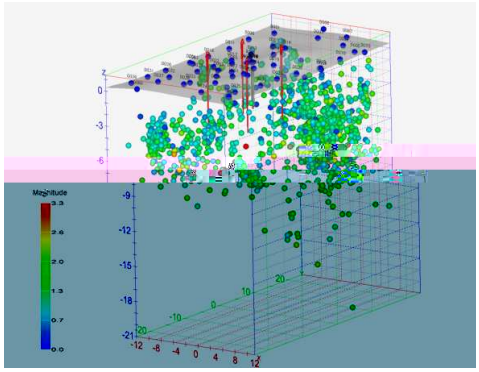

Fig.2 Events used for the PST.

From the acquired dataset, 1860 events (Fig.2) were selected to be used in the tomographic inversion. Magnitudes of the located events range from 0-3R with the majority of them between 1-2R.

Hypocentral depths are between 0-20km while most of them are between 2-10km. Most of the events have been located using 10-30 P- and S- wave arrivals and their RMS errors ranged from 0-0.15sec.

The data processing of a PST survey can be divided into three main steps. The first one is the estimation of the best-fitting 1D initial velocity model in parallel with the optimization of the hypocentre locations. The second is the 3D velocity model construction and the third is related to the quality control of the results. The aim of PST inversion is the estimation of a 3D velocity model and the corresponding hypocentre parameters, having as known parameters only the arrival times of the P- and S-waves at the seismic stations, a first estimation of the hypocentre locations and the positions of the seismic stations (all with some uncertainty). A detailed description of the data processing methodology is presented in Martakis et al., 2006; and Tselentis et al., 2007.

The seismic events used provided a total of 47280 P and S-wave arrivals, (24438 P and 22842 S-wave arrivals), that were used for the tomographic inversion in order to estimate 25076 V_p and V_p/V_s parameters. The final model RMS was 0.0964, reduced by 21.5 % from a

starting value of 0.1228. The final total RMS for seismic events hypocentral estimation was 0.070, reduced by 39.1% (from a starting value of 0.115).

Results

In the present paper we will not make detailed geological/lithologic interpretation of the PST results. The quantitative interpretation of PST results in relation to the properties of hydrocarbon reservoir is a complicated task and will be the scope of a separate paper.

Fig.3 compares the obtained V_p cross-section along DD' (Fig.4), with a geological model given by the Albanian Natural agency of Hydrocarbons, (Vellaj, 2001 and Luan et al 2001). Judging from this figure, it is obvious that geological and tomography data are correlating very satisfactory. Starting from the West, the low velocities (a) correspond to quaternary and flysch deposits and high velocities (b) fit very well with Cretaceous, Jurassic and Tertiary outcrops towards the NW part of the investigated region. The anticline (c) is also reconstructed very well and the Evaporitic-flysch (d), T3, Tertiary dolomites (e) and Jurassic Carbonates (f) layers correlate also very well by the velocity section from PST. This correlation is presented as an additional QC test and not for interpretational reasons. Fig. 5a,b depicts vertical V_p and V_p/V_s sections respectively, while similar horizontal sections at 1Km spacing are presented in Fig.6a,b.

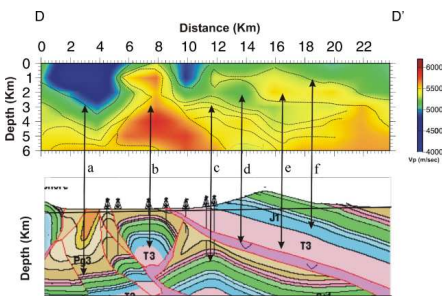

Fig.3. Comparison with Geology

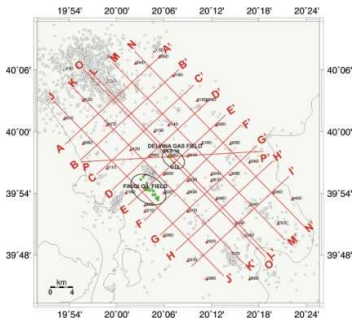

Fig.4. Cross sections

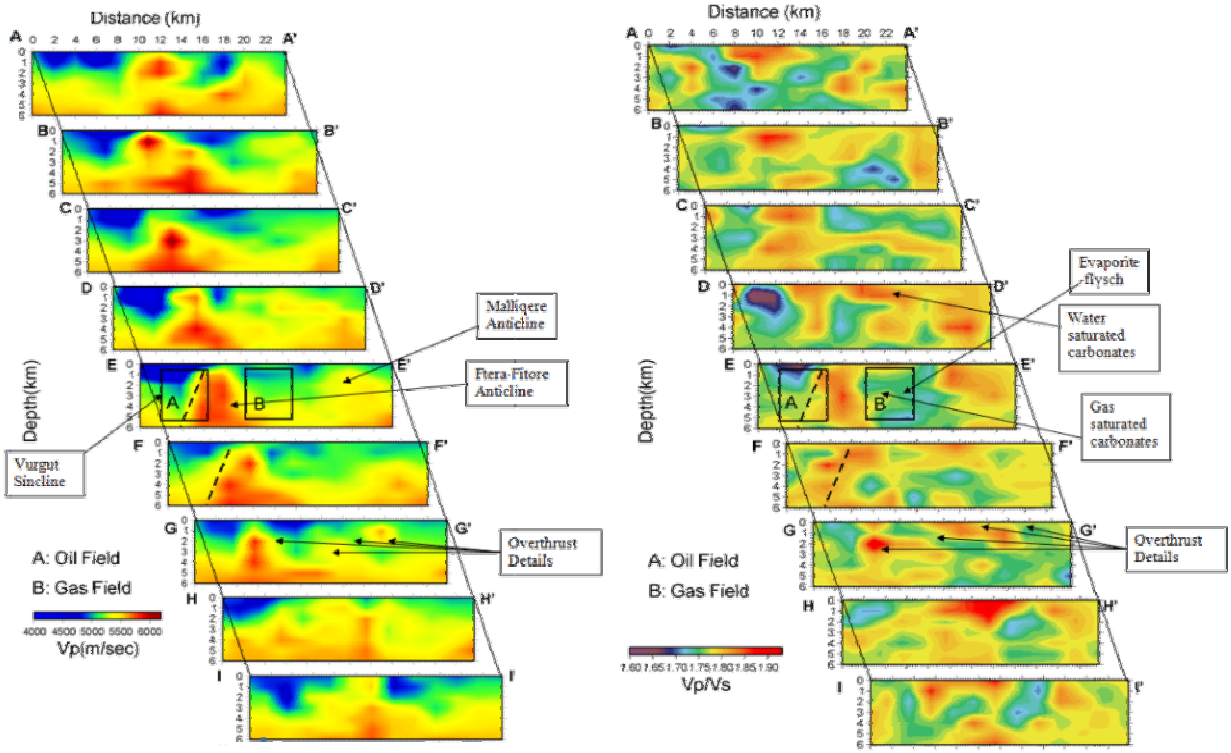

Fig.5. Vertical sections of (a) V_p and (b) V_s

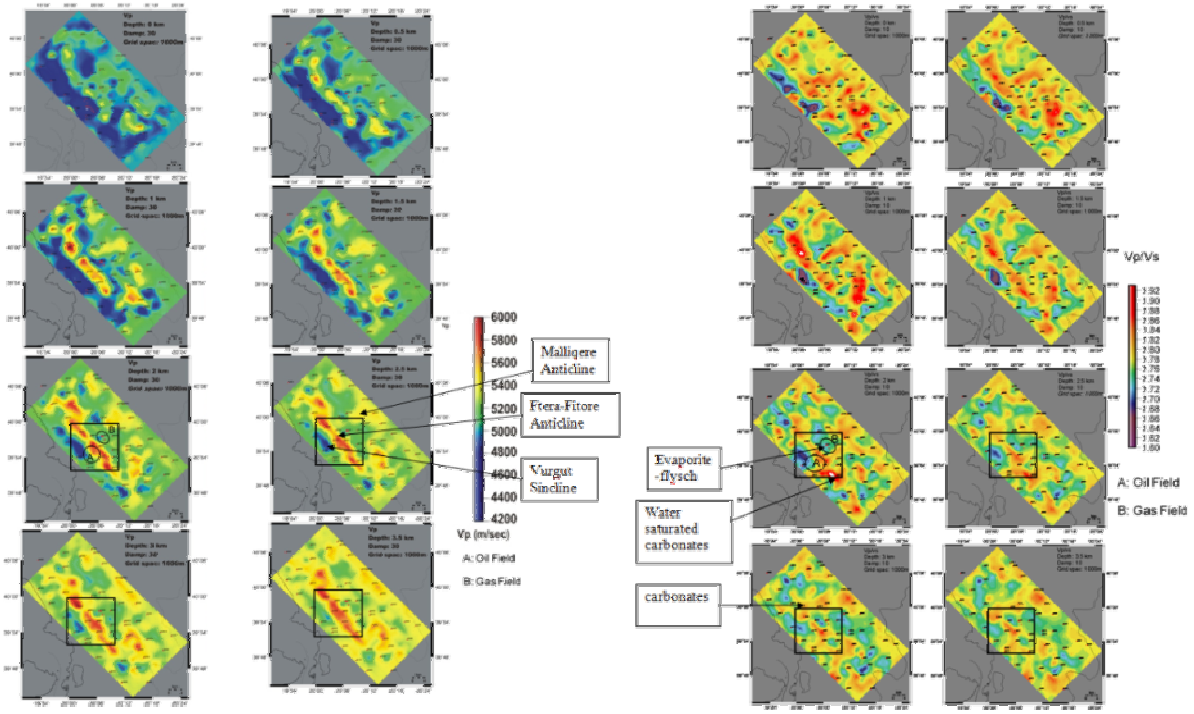

Fig.6. Horizontal sections of (a) V_p and (b) V_p/V_s.

Apart from the structural information given by the V_p and V_p/V_s sections, some lithological information can also be obtained. It is known that V_p is sensitive to the saturation fluid type. The use of the ratio of V_p/V_s is a good tool in identifying fluid types. The fact that V_p decreases and V_s increases with the increase of light hydrocarbon saturation, makes the ratio V_p/V_s more sensitive to change of fluid type than use of V_p or V_s separately.

Within the area of investigation there are one gas and one oil producing reservoir (region A, B in Fig.5, 6 respectively). Judging from the V_p and V_p/V_s tomographic data along EE' cross-section which passes throughout the centre of the oil field (Fig.5), we can see that the oil reservoir is trapped between an anhydrite formation to the SW and a thrust fault rising the flych formations to the surface (fault 3-way closure with anhydrite top seal). Similar results can be seen at the horizontal tomographic sections of Fig.6.

Fig.7a, b depicts the obtained values of V_p/V_s versus V_s and V_p respectively, for the oil producing region for various depths. Judging from this diagram we can see that at the depth that the oil reservoir is encountered (~2Km), the V_p/V_s values reach a maximum in contradiction to the minimum values obtained for the gas field.

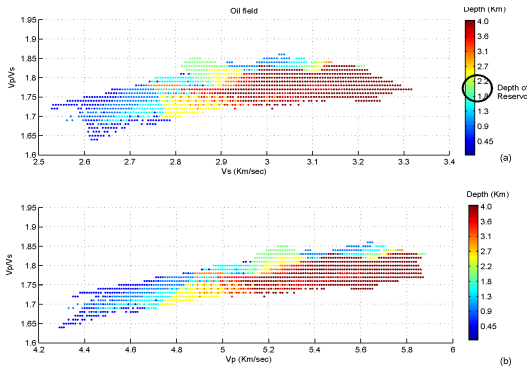

Fig.7. V_p/V_s versus (a) V_s; (b) V_p.

A detailed presentation of the Vp/Vs results along section EE' is depicted in Fig.8. EE' passes through Finiq Oil Field and D12 well in Delvina Gas field. Low Vp/Vs values (1-65-1.75) corresponds to low porosity formations.

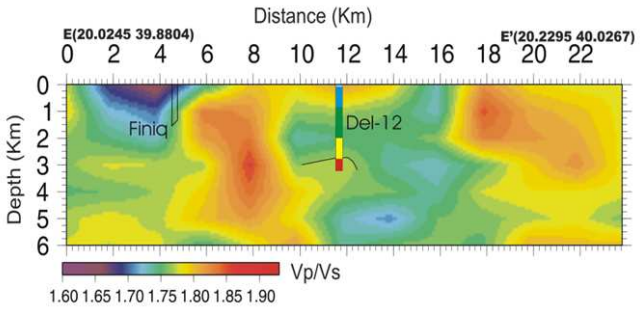

Fig.8. Vp/Vs results versus depth along EE'.

Especially for evaporites and flysch (based also on well information) the V_p/V_s values range from 1.70-1.75 (blue to green colors) and for carbonates from 1.76 -190 (yellow to red colors). V_p/V_s values 1.76-1.77 correlate very well with gas saturated carbonates and very high values 1.86-1.90 can be justified from water saturation of high porosity carbonates.

Apart from the above mentioned general PST results, in the following figures we present an interpretation of PST results by correlation with pre-existing geological, geophysical and well data focusing mainly on Delvina Gas Field Area. In Fig.9a, b the correlation between PST and pre-existing data is presented in 2 and 3.5 km respectively. In both figures the correlation is very good for most of the structures (Ftera-Fitore, Maliqere anticlines and Vurgut Sincline). Finiq oil field can also be identified although it is a small structure. In Delvina Area the correlation is good but based on PST results the Delvina anticline structure would be expected in NWN-SES direction rather than NW-SE based on the pre-existing data interpretation (20^o clockwise difference).

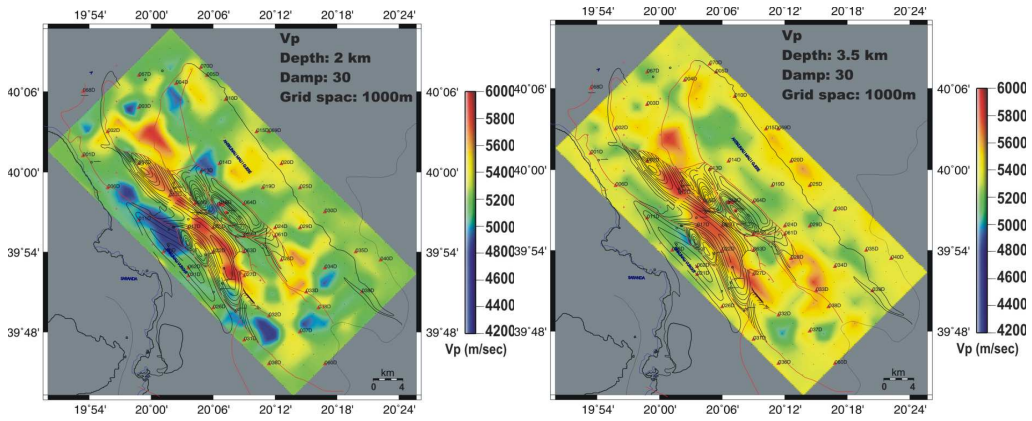

Fig.9. Comparison of PST results with known structure at (a) 2Km and (b) 3.5Km.

In Fig. 10 we present a 3D view of the Delvina Anticline structure and the surrounding structures as proposed by Passive Seismic results. As a conclusion, it can be seen that the Delvina Anticline is an adjacent structure to the anticline structure Ftera-Fitore (towards West).

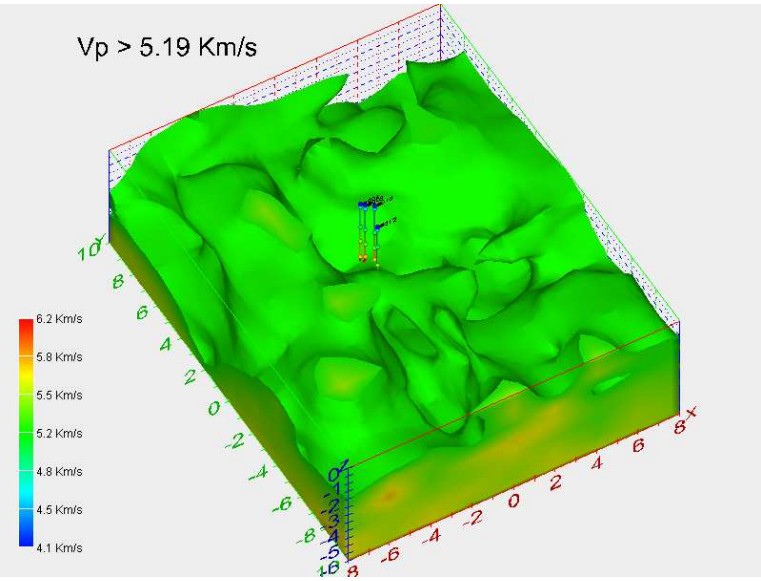

Fig.10. 3D view of Delvina anticline structure and the surrounding structures based on Passive Seismic results (V_p>5.19). The production wells are on top of the anticline structure.

Conclusions

The passive results showed satisfactory correlation with the geological features and the production characteristics of the existing wells in the area, and they explained the lateral distribution of the oil and gas reservoirs. Based on comparison between conventional seismic and PST it is obvious that information provided by PST especially in the area of interest is superior to conventional seismic (even comparing to the earliest 2D seismic results of 2001). The very complicated, overthrusted geotectonical regime along with the presence of evaporitic structures are the reasons for poor quality conventional seismic and at the same time are the reason that make PST as the most appropriate method for this area (even having in mind its limitations).

References

N. Martakis, S. Kapotas and G-A. Tselentis, 2006, *Integrated Passive Seismic Acquisition And Methodology. Case Studies*. Geophysical Prospecting, **54**, 829–847.

S.C. Maxwell and T.I. Urbancic, 2001, *The role of passive microseismic monitoring in the instrumented oil field*. *Leading Edge*, **20**, 636–639.

G-A. Tselentis, A. Serpetsidaki, N. Martakis, E. Sokos, P. Paraskevopoulos, and S. Kapotas, 2007, *Local high resolution passive seismic tomography and Kohonen neural networks, application at the Rio-Antirrio Strait, Central Greece*. Geophysics, **72**, (4) B93-B106.

H. Zhang, S. Sarkar, M. N. Toksoz, H. S. Kuleli, and F. Al-Kindy, 2009, *Passive seismic tomography using induced seismicity at a petroleum field in Oma*n. Geophysics, **74**, WCB57-WCB69.